

23 Prediction of GNSS Availability and Accuracy in Urban Environments – Case Study Schiphol Airport

Frank Kleijer¹, Dennis Odijk² and Edward Verbree¹

¹ Delft University of Technology, OTB Research Institute for Housing
The Netherlands

² Delft University of Technology, Department of Earth Observation and
Space Systems, The Netherlands

Abstract

Because of the increased call for positioning in urban areas, the performance of GNSS is analyzed under conditions with a decreased satellite visibility caused by buildings blocking the lines of sight. With GPS and Galileo almanacs and two city models visibility fingerprints of time–location combinations are computed. Outdoor availability and accuracy are predicted for both city models: Real-life data of Schiphol Airport, and an imaginary urban canyon model (located in the same area as Schiphol) with variable parameters for street width, street length and building block height. The accuracy is predicted based on dilution-of-precision values. GPS, Galileo, and a combined constellation are considered for single-frequency single-epoch positioning.

Even for mildly difficult urban environments 95% availability is not reached for GPS (or Galileo) close to buildings or in streets in north-south directions. In the combined GPS-Galileo constellation a substantial improvement of 30%–50% availability can be reached as compared to GPS only for those locations where GPS availability is already more than ~10% (under severe conditions such a high increase cannot be achieved). At Schiphol Airport, however, conditions are very mild since there are only a few enclosed areas, surrounded by more than one building block and in most vital areas 95% availability can be reached even with GPS only. The accuracy close to the buildings and piers is, on average, decreased however, up to a factor of about three very close to buildings. This effect is even larger on the south-west and south-east side of buildings because there the high satellite density in north-east and north-west directions cannot be exploited.

Keywords: Global Navigation Satellite Systems (GNSS), line of sight (LOS), dilution of precision (DOP), availability, Schiphol Airport

23.1 Introduction

With the advent of the Global Positioning System (GPS) positioning has become daily practice for many vehicles as well as increasingly so for pedestrians. Ever more new location-based services (LBS) are being developed based on GPS. Advantages of GPS over other techniques are that it is operational, global, 3D, accurate, and relatively cheap. Besides, in principle, no additional infrastructure of reference points, transmitters and/or receivers is needed by providers of location-based services, although they may choose to provide such an infrastructure, e.g., by assisted GPS. Nevertheless, accurate and independent positioning at any time and at any place in urban environments is still problematic. In urban environments, where positioning needs are often most present, the GPS signals are being blocked or attenuated and often are received via multipath signals. This means that both availability and accuracy of GPS are seriously harmed. With availability (Swan et al. 2003, Verbree et al. 2004) we mean the percentage of time that a sufficient amount of satellites are visible, or, in other words, a sufficient amount of satellites have unblocked direct lines of sight (LOSs). In combination with Galileo, the future European Global Navigation Satellite System (GNSS), both availability and accuracy will increase.

In this paper we study to what extent the shielding of signals by buildings degrades the availability and accuracy of both GPS and Galileo single-point positioning as well as the combination of both systems (G2). For this we used two models: A simple but very instructive urban canyon model with variable parameters that we could easily construct ourselves, and a real-life model in the Netherlands of Schiphol Airport with rooftops of terminals, piers, parking garages, and other buildings that we received from the Schiphol Group as Autocad data based on terrestrial surveys. Unlike previous work (Verbree et al. 2004, Tiberius & Verbree 2004, Liu et al. 2006, Taylor et al. 2007) related to our topic we were therefore not concerned with gathering data and how to do that. Also we were not concerned with LOS computations given a certain digital terrain model because we assumed flat streets in the urban canyon model and a flat terrain at Schiphol Airport. In the latter model, a flat terrain was close to reality for most of the area.

With the urban canyon model we focus mainly on understanding GNSS availability under different urban conditions, taking into account street width, building heights and receiver location. It has a typical shape where GNSS signals are blocked by buildings on two sides of a street. Accuracy was predicted for one set of city model parameters.

The other model is more open: LOSs are at most areas blocked from one side only, and in some areas at three sides. Schiphol has been an interesting case study because it is often considered a small city where 24 hours a day activities take place, and because it has a high potential for LBS. Many applications are under consider-

ation by the Schiphol Group, both indoors and outdoors. This paper is a report of a partial project where we only consider the GNSS outdoor case; the GPS indoor case is treated by Odijk and Kleijer (2007) and Odijk and Kleijer (2008).

Outdoor positioning at Schiphol may be done for navigation, tracking & tracing, or just for recording coordinates. Procedures can be improved by positioning of personnel, vehicles, passengers, luggage, materials, and incidents. Personnel that may benefit from personal positioning are, e.g., security personnel, authority officers, firefighters, and emergency services. These personnel will have a need for positioning in vehicles as well. Vehicle positioning is important for basically all vehicles on the runway, but also for many vehicles on the platform and on landside. One may think of luggage trolleys, airplane lorries, grit sprinklers, street cleaning cars, mowing machines, etc. Registration of incidents is important to improve compliance: Reports of incidents are made for analyses to detect trends. For these reports coordinates need to be recorded accurately and on the spot with simple devices, e.g. in case of possible environmental pollution. From interviews with employees of the Schiphol Group it became clear that for many applications a 10m accuracy is sufficient. For some special cases, however, higher accuracy is advisable.

Our approach to LOS computations is given in *Section 23.2*. The GPS and Galileo availability are studied in *Section 23.3* for both data sets. In *Section 23.4* the attainable accuracy in the two models is studied by means of dilution-of-precision (DOP) values. *Section 23.5* concludes this paper.

Table 23.1. GPS and Galileo system characteristics.

GNSS	GPS	Galileo
Status	Operational	Planned
Number of orbits	6	3
Number of satellites	24	27 + 3
Inclination	55°	56°
Semi-major axis	26560 km	29600 km
Period	11 h 58 min	14 h 4 min 42 s
Ground track repeat	10 days / 20 orbits	10 days / 17 orbits

23.2 Line-Of-Sight Computations

With GNSS almanac data and a given 3D city model one can predict which satellites are visible at a certain receiver position in that city model. In other words, if there is a building blocking the LOS, one can predict that no signal or a much weaker signal will be received. Almanacs contain information about which satellite is where at which time. For this study a software tool was created with which we

did LOS computations based on both GPS and Galileo almanacs. Some characteristics of both systems are given in *Table 23.1*. For the GPS LOS computations we used a Yuma almanac (<http://www.navcen.uscg.gov/gps/default.htm>) of GPS week 328, December 2005. For the Galileo LOS computations an almanac was used that was created (Verhagen et al. 2002) based on a 27/3/1 Walker constellation (Walker 1984). In these almanacs there were 29 GPS satellites, slightly more than the nominal constellation, and 30 Galileo satellites. Unless stated otherwise, for the computations of sections 3 and 4, satellite coordinates were determined for 96 epochs with a separation of 2.5 hours spanning 10 days. This choice was made to have a homogeneous spread of satellite constellations for GPS, Galileo, as well as for the combination (the ground track repeat differs for GPS and Galileo, see *Table 23.1*) without the need of high computing power (and therefore long calculation times). In the LOS computations we only considered satellites with an elevation cut-off angle above 10° because in real-life circumstances such a cut-off angle would make sense as well to avoid multipath signals.

All visibility information of satellites at a certain epoch for a certain receiver location is considered to make up a GNSS fingerprint of an epoch–location combination. For each of the 29+30 satellites the result of a LOS computation is either:

1. The LOS is not blocked.
2. The LOS is blocked.
3. The LOS is below the elevation cut-off angle.

Satellite coordinates are computed in earth-centred earth-fixed (ECEF) WGS-84 coordinates (X_s, Y_s, Z_s) . However, we found it easier to do the LOS computations in a local 3D Cartesian coordinate system. Horizontal coordinates (x, y) of the Schiphol data set were available in the Dutch RD (Rijks Driehoeksmeting) system. These are Cartesian map coordinates roughly corresponding to easting and northing. Vertical coordinates (heights H) were given in NAP (Normaal Amsterdams Peil or Amsterdam Ordnance Datum). Strictly speaking the combined coordinates are not Cartesian, but for a small area we can consider them as such. Receiver coordinates were chosen at locations in the RD-NAP system (x_r, y_r, H_r) .

In order to do LOS computations in RD-NAP, we computed pseudo-satellite coordinates close to the city model $(X_{\bar{s}}, Y_{\bar{s}}, Z_{\bar{s}})$ in such a way that they are still on the same LOS from receiver to satellite; compare (Taylor et al. 2007). For this purpose the chosen receiver coordinates were transformed to WGS-84 coordinates: $(X_r, Y_r, Z_r) \leftarrow (x_r, y_r, H_r)$. These WGS-84 coordinates were also used to compute elevation angles and to do DOP computations. Then pseudo-satellite coordinates were derived as $(X_{\bar{s}}, Y_{\bar{s}}, Z_{\bar{s}}) = (X_r, Y_r, Z_r) + (X_{rs}, Y_{rs}, Z_{rs}) \cdot \bar{\rho} / \rho$, where $\cdot_{rs} = \cdot_s - \cdot_r$, and ρ and $\bar{\rho}$ are the ranges from receiver to satellite and pseudo-satellite respectively. The range $\bar{\rho}$ is chosen such that the pseudo-satellite position lies just outside or on a bounding box around the city model. The pseudo-satellite coordinates are then

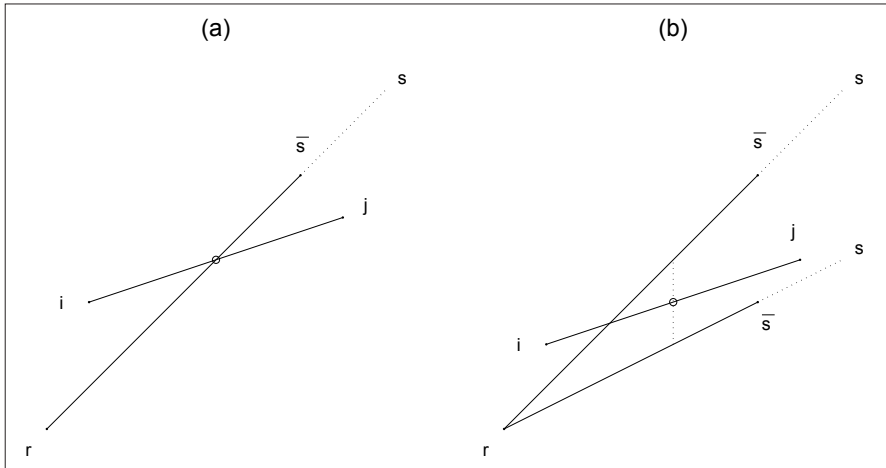


Fig. 23.1. Illustration of LOS computation for receiver r , satellite s and pseudo-satellite \bar{s} . (a) If in 2D the projection of the LOS ($r; s$) or ($r; \bar{s}$) crosses the projection of the rooftop edge (i, j) at the point indicated with ‘o’, the height of the LOS at that point is computed as well as the height of the line (i, j). (b) If in 3D the LOS ($r; s$) is above (i, j) the LOS is unblocked, else it is blocked.

transformed to RD-NAP: $(x_{\bar{s}}, y_{\bar{s}}, H_{\bar{s}}) \leftarrow (X_{\bar{s}}, Y_{\bar{s}}, Z_{\bar{s}})$. The transformations were done in two steps, using the equations by Bowring (1976) for transformation between ECEF coordinates and ellipsoidal coordinates (using the WGS-84 ellipsoid), and the equations by Schreutelkamp and Strang van Hees (2001) for transformation between ellipsoidal coordinates and RD; a geoid height of 43.1 m was assumed (De Min 1996). Although the latter transformation is an approximation (95% of the coordinates lie within 15 cm), it is considered sufficient for our purpose.

Once the pseudo-satellite coordinates in the RD-NAP system are obtained, they are used for the LOS computations in the following way (see *Figure 23.1*):

1. A 2D intersection is computed for each 2D rooftop polygon edge ij with coordinates (x_i, y_i, H_i) and (x_j, y_j, H_j) that potentially blocks a LOS $(x_r, y_r, H_r) - (x_{\bar{s}}, y_{\bar{s}}, H_{\bar{s}})$.
2. If there is an intersection, the height of the LOS at the intersection is compared with the height of the line ij at that intersection. If the line ij is higher than the LOS, the LOS is blocked, else it is not blocked by ij (but possibly by another rooftop line).

Although this is basically a very simple computation, computation costs will grow considerably with increasing amounts of rooftop edges, satellites, epochs, and receivers. Computation time was therefore limited by reducing the amount of potentially blocking rooftop lines: In a preprocessing step pointers were created pointing to all 2D rooftop edges in an artificial 2D grid cell, and in step 1 above only those grid cells were considered that cross the LOS.

23.3 GNSS Availability

Based on the GNSS fingerprints obtained from the LOS computations we can predict whether it is possible to compute the receiver coordinates. In a constellation with only GPS or Galileo satellites four satellites are needed for single-epoch (real-time) positioning because there are three coordinates and one receiver clock bias to be computed. In a constellation with both GNSS systems we assume there is an extra parameter to be determined: the time offset between GPS and Galileo (although in practise this might not be needed if this offset is sufficiently small or when information on this offset can be retrieved externally). In this case we need either two GPS satellites and three Galileo satellites, three GPS satellites and two Galileo satellites, or four satellites of either GNSS. The percentage of time that a sufficient number of satellites are visible we call availability. The availability of GPS, Galileo, and G2 is computed for both the urban canyon model and the Schiphol Airport data.

Bradbury et al. (2007) stressed that the urban environment is a multipath rich environment where one should take into account reflections and diffraction effects for computing availability. In our computations we did not take multipath into account, not only because of its complications, but since we are not particularly interested in specific time-location satellite availability but rather in availability expressed in percentages of time. It is unlikely that multipath is responsible for very different availability numbers as derived here for conventional (i.e. non high-sensitivity) GPS receivers since many receivers are mostly sensitive to short-delay multipath and many techniques are developed to suppress long-delay multipath; see, e.g. Sleewagen and Boon (2001). For high-sensitivity receivers however we see possible added value in using city models for predicting availability based on reflections as well. As shown by Bradbury (2007), because of diffraction, satellites may appear visible for a longer time (~5–10 minutes) than predicted based on direct LOS computations when setting behind a building or earlier when rising behind a building. Availability may therefore increase by diffraction. Considering a satellite that is being blocked twice per pass (when rising and setting) satellite visibility may then increase with ~5% of the total time for a satellite that is above the elevation cut-off angle for 5 hours. Availability may decrease however by line-of-sight blockage by cars, trees, and other objects.

23.3.1 The Urban Canyon Model

The urban canyon model is made up of twelve building blocks with streets in between. The four central building blocks are shown in *Figure 23.2*. In each of the cardinal directions two extra building blocks are located to represent a continuation of an infinitely large Manhattan-like city with equal building blocks. The model has three parameters: a street width w , a street length l , and a building block height

H (street heights are 0 m+NAP). Typical values for the street widths and building block heights are given in *Table 23.2*. As central location for the model we chose (arbitrary) coordinates from the Schiphol Airport area ($x=113200$ m, $y=480250$ m; corresponding to approximate latitude 52.31° N, and longitude 4.77° E). Availability numbers were computed for 65 locations in the model. Of these locations 23 are shown in *Figure 23.2*. Because the results were highly symmetrical (especially in east-west direction), only the results of 21 locations in the corner south-east of the central location 17 plus two additional locations are shown in *Figure 23.3*.

Table 23.2. Urban canyon model parameters used for the results of *Figures 23.3* and *23.4*.

height	8 m	regular house
	15 m	mansion
	30 m	low block of flats
	100 m	high block of flats
width	5 m	alley
	20 m	regular street
	80 m	open area

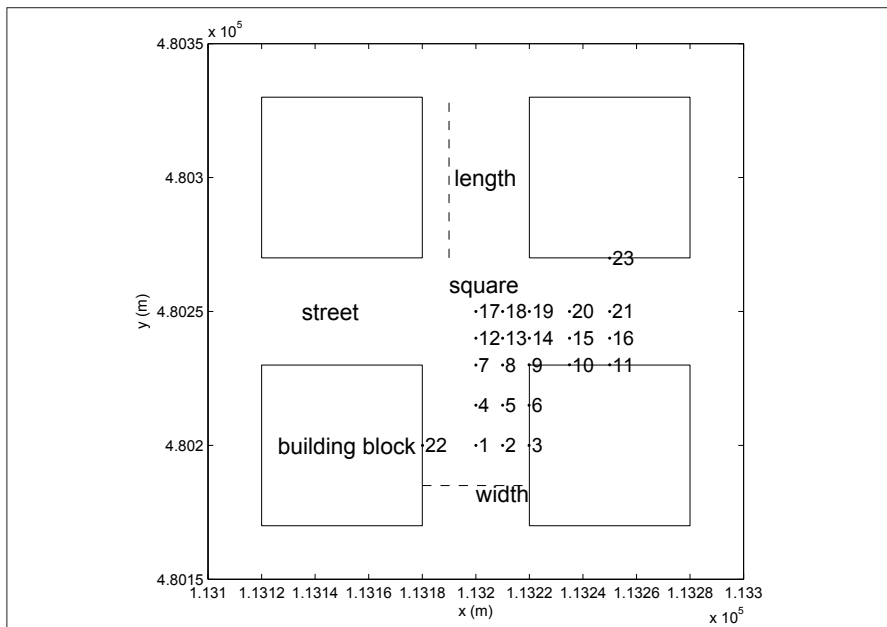


Fig. 23.2. Receiver locations used for the availability analyses in the urban canyon model. The locations 1, 4, 7, 12, and 17–21 are on the axes of the streets; locations 3, 6, 9–11, 22, and 23 are located 10 cm from the walls; locations 2, 5, 8, and 13–16 are at one (three) quarter of the street width; locations 1–3, 11, 16, and 21–23 are halfway the street length; locations 4–6, 10, 15, and 20 are at one (three) quarter of the street length.

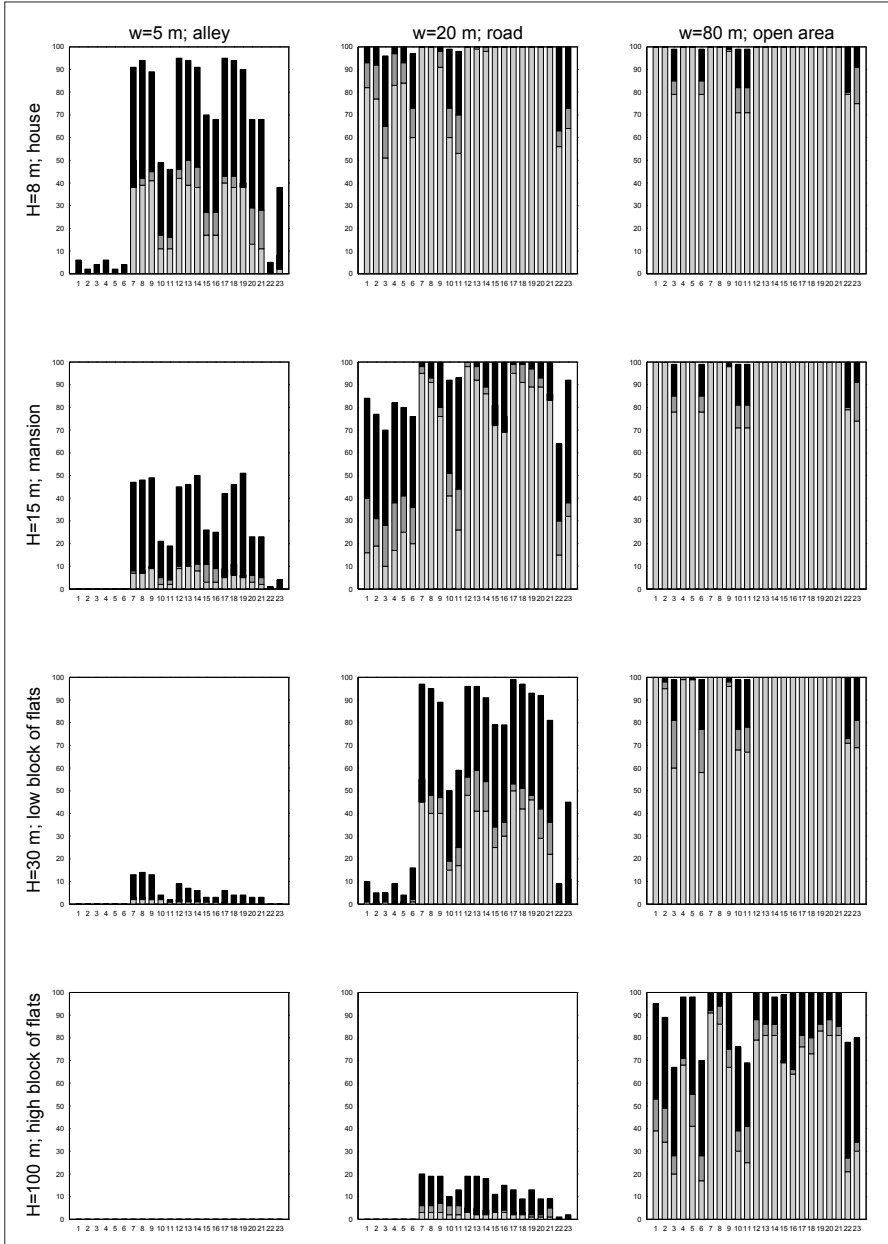


Fig. 23.3. Visibility percentages for the 23 locations of *Figure 23.2* in the 12 urban canyon scenarios (width $w = 5, 20, 80$ m; height $H = 8, 15, 30, 100$ m). Light grey: GPS only. Light grey plus dark grey: Galileo only. Total bar length: GPS + Galileo.

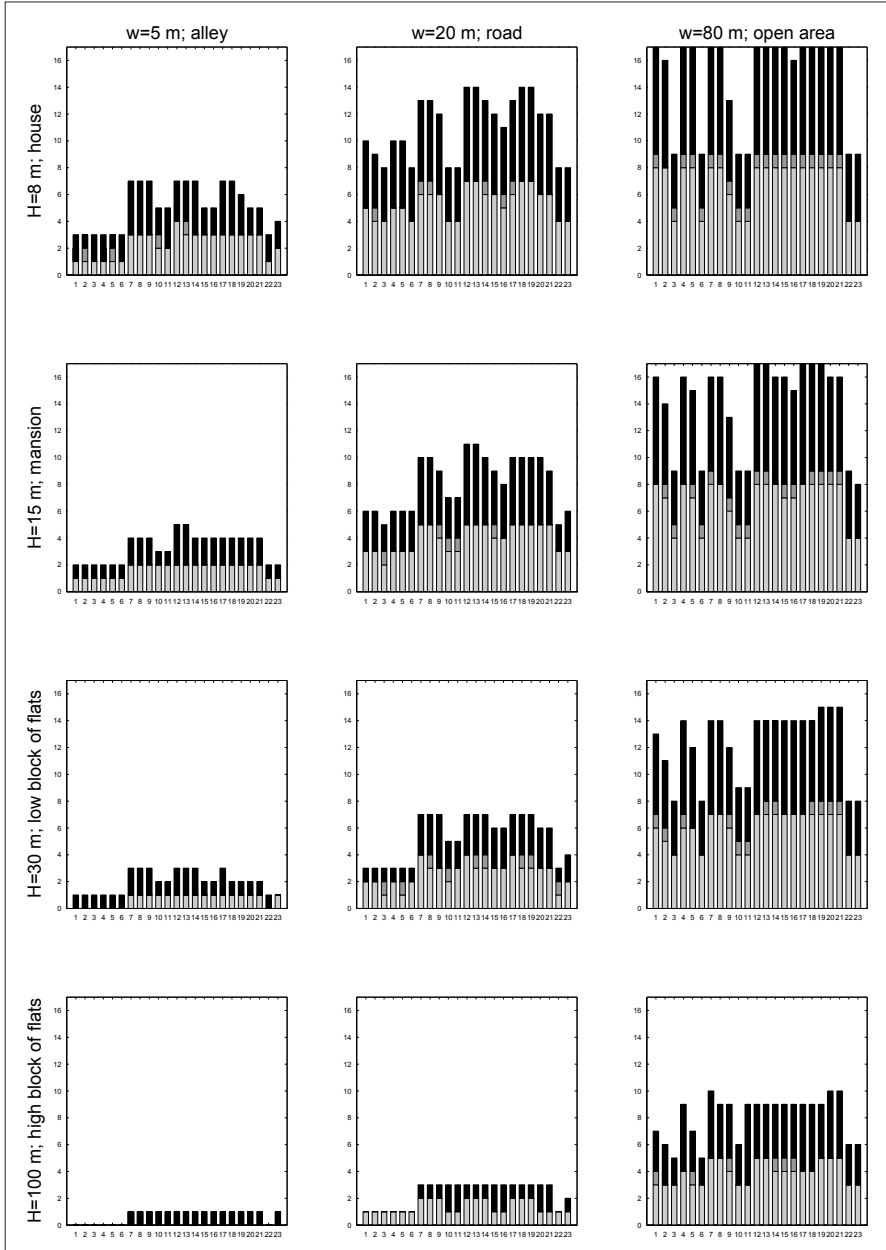


Fig. 23.4. Average number of visible satellites (rounded to integers) corresponding with the scenarios of *Figure 23.3*. Light grey: GPS only. Light grey plus dark grey: Galileo only. Total bar length: GPS + Galileo.

Figure 23.3 shows the results for twelve different models with each combination of building block height and street width as indicated in *Table 23.2*. Because the model showed little dependence on the street length we fixed it to one value: 50 m. *Figure 23.4* shows the average number of satellites on which *Figure 23.3* is based.

In order to help interpretation of *Figure 23.3*, *Figure 23.5* gives an impression of GPS satellite visibility for the central location 17 with model parameters $w = 20$ m and $H = 15$ m. *Figures 23.6* and *23.7* only show the rooftops to illustrate the effect of different model parameters and locations. These down-looking skyplots preserve azimuths, whereas zenith angles are represented by radial distances to the centre. In the centre the receiver position is shown by a + sign. The dashed lines represent the 80° zenith cut-off angle (the angle between the zenith and LOS) which corresponds with an elevation cut-off angle of 10° . All satellite positions in the 96 epochs used are shown in *Figure 23.5*. The solid lines represent the rooftops and walls of the buildings. When the elevation angle of a satellite is lower than the elevation angle of a rooftop the satellite is not visible. This translates in the skyplot as non-visibility when the radial distance of a satellite is larger than any rooftop edge. There is a clear lack of satellites in the northern part of *Figure 23.5* caused by the 55° inclination of the orbits. The specific location of such a hole depends on the latitude. The hole causes visibility and availability to be lower in north-south streets than in east-west streets. Also, a receiver location against a wall decreases visibility and availability considerably. This is especially so under mild conditions (low H/w) because the decrease in solid angle of clear sky visibility is more pronounced.

Figure 23.3 shows that Galileo has slightly higher availability numbers than GPS in most of the cases (the rare cases where this is not so are not shown). This may be caused by the satellite geometry as well as the additional satellite in the almanac. In the combined geometry availability values show a steep increase for those situations where availability for GPS or Galileo is already more than $\sim 10\%$. An increase of 30% – 50% of availability of G2 with respect to GPS-only can be seen for several locations. This increase agrees with the numbers given in (Swan et al. 2003) who claimed 56.3% availability for roads in Stuttgart and 99.7% for G2. Also it is confirmed that a higher value can be found for Galileo (78.3% in the Stuttgart case), although it would probably go too far as to say that Galileo would perform better in general. For availability values below $\sim 10\%$ the buildings are often blocking so much of the sky that extra satellites do not help much. A high increase can be seen, for example, for squares of alleys with houses or mansions, 20 m wide roads with mansions, and high blocks of flats in open areas. The increase is especially notable for those situations where the average number of satellites increases from below four to more than four.

In order to rely on GNSS, for many applications one would like to have at least 95% availability. An availability of 95% or higher for either GPS or Galileo can be seen for 20 m wide east-west roads with regular houses, but not against walls or in north-south streets, and for Galileo also at the centre of squares surrounded by

mansions. For open areas surrounded by mansions also 95% can be reached, but not close to walls. At least about seven visible satellites on average are needed to reach this availability. In the G2 situation with 20 m wide roads and regular houses 95% is always reached. With mansions only at squares and east-west streets, but not against walls. With low blocks of flats this percentage is only reached at the centre of squares. G2 with open areas give 95% availability for mansions, even against walls, and for low blocks of flats if the receiver is not located against the wall. For alleys, only at the centre of squares and with regular houses, 95% can be reached.

A visibility of 5% or lower is seen for alleys with low blocks of flats, mansions if not at a square, or regular houses in streets in north-south direction. For regular streets this percentage is seen for high blocks of flats and streets surrounded by mansions in north-south streets.

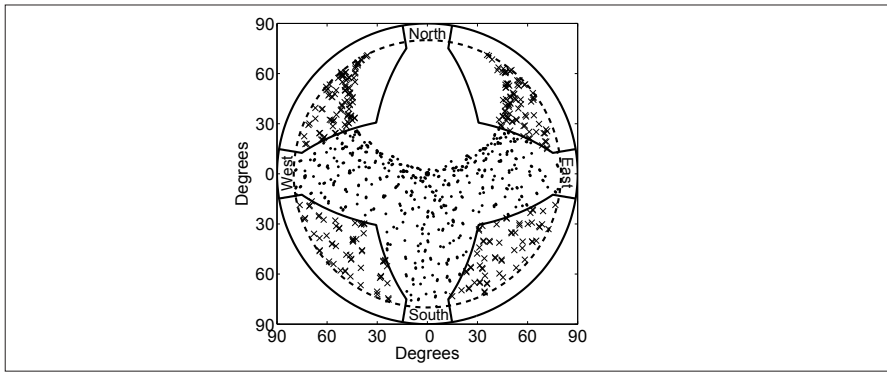


Fig. 23.5. GPS skyplot for the urban canyon model with parameters $H = 15$ m and $w = 20$ m, and for receiver location 17 (central location). Dots represent visible satellites; crosses represent non-visible satellites.

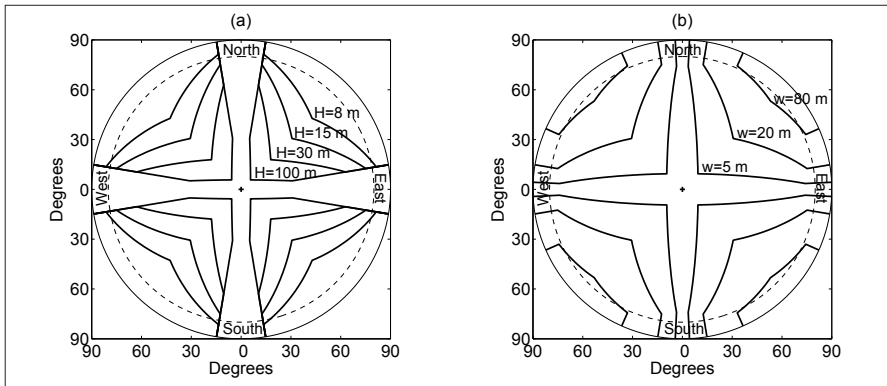


Fig. 23.6. Skyplots of rooftops in different versions of the urban canyon model. Receiver location 17 (central location). (a) Parameters: $w = 20$ m; $H = 8, 15, 30, 100$ m. (b) Parameters: $H = 15$ m; $w = 5, 20, 80$ m.

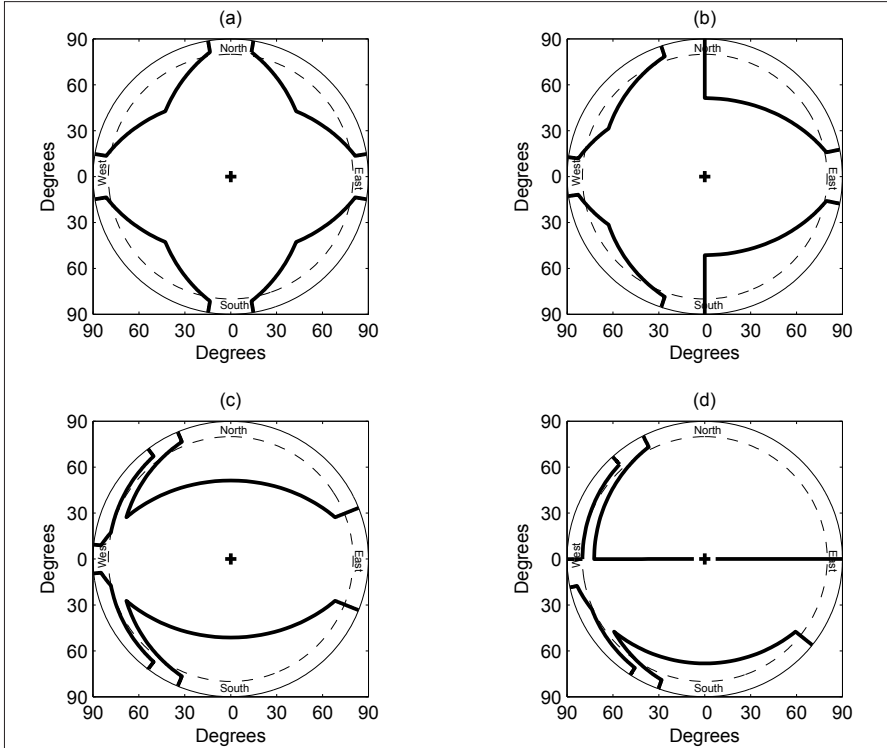


Fig. 23.7. Skyplots of rooftops in the urban canyon model for four different locations. Parameters: $H = 8$ m; $w = 20$ m. Receiver locations: 17 (a), 19 (b), 21 (c), and 23 (d).

23.3.2 Schiphol Airport

For the Schiphol dataset availability percentages were computed at a height of -3 m +NAP for every 10 m grid cell in the GPS-only, Galileo-only and G2 situation. *Figures 23.8* and *23.9* show the GPS and G2 cases respectively (the Galileo-only case was very similar to the GPS-only case). Only if an availability lower than 95% was reached a red area was plotted. In black are shown the building blocks as well as areas for which no availability was computed because the cell centres fell inside building polygons.

From these plots we can conclude that for the areas around the piers over 95% availability can be reached even in the GPS-only case. This can be expected since only on one side the signals are being blocked, which is comparable with the urban canyon model for open areas. Only around high buildings with more than one blocking side availability is lower. This is the case at some buildings of the Schiphol Group; but these are not the vital places for GNSS use.

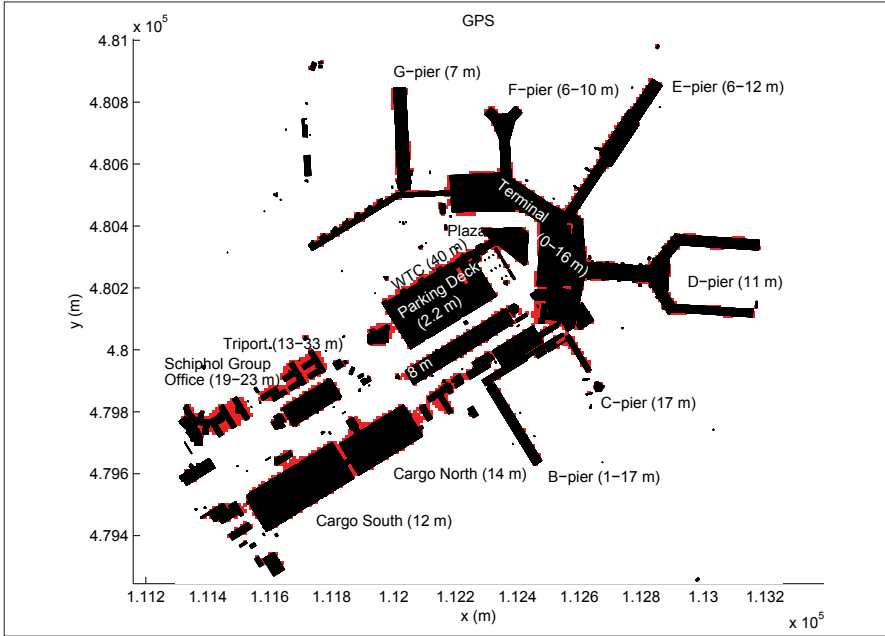


Fig. 23.8. GPS availability at Schiphol Airport. Red: Less than 95%. White: More than 95%.

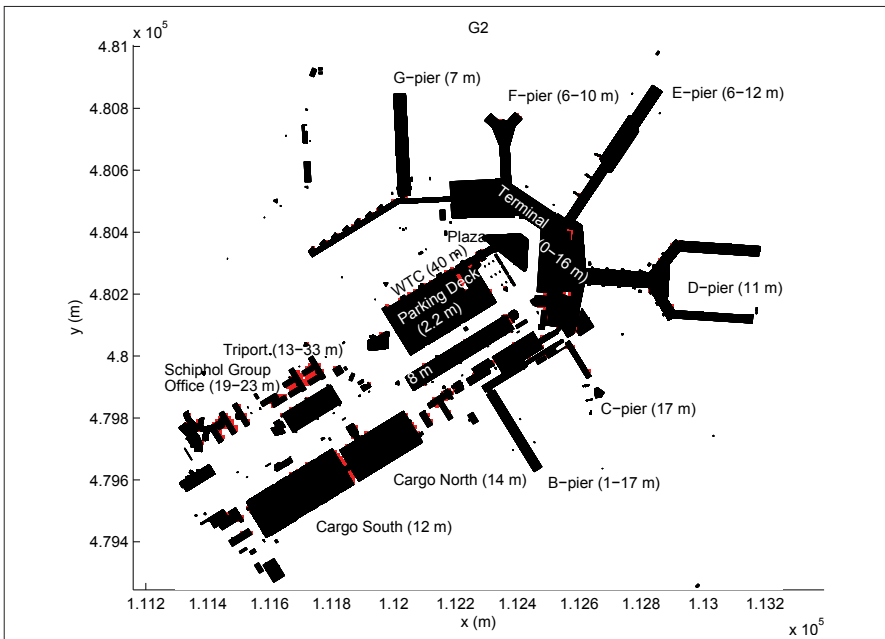


Fig. 23.9. G2 availability at Schiphol Airport. Red: Less than 95%. White: More than 95%.

23.4 GNSS Dilution of Precision

In this section we deal with the accuracy that is achievable with one epoch of observations using either GPS, Galileo, or G2 under urban conditions. We do this by comparing dilution-of-precision (DOP) values. We can distinguish, amongst others, a vertical, horizontal, and position DOP, which are indicated by VDOP, HDOP and PDOP respectively. These dimensionless values are derived from the covariance matrix of the parameters assuming an identity matrix for a covariance matrix of the observations; see, e.g., (Hofmann-Wellenhof et al. 1992) for a discourse on how to do the computations. The covariance matrix of the parameters depends on the satellite geometry including the number of satellites, and the precision of the GPS observations. For practical purposes the covariance matrix of the observations is often assumed to be a diagonal matrix scaled with a variance scale factor. The square root of this scale factor is called user-equivalent range error (UERE), which depends on several error sources. A realistic computation of the UERE for GPS observations on one frequency is given in *Table 23.3*. In this table we also took into account the effect of multipath/diffraction.

Table 23.3. Error contribution to the UERE.

Error	st. dev.	variance
Ionosphere	4.0 m	16.00 m ²
Ephemeris	2.0 m	4.00 m ²
Satellite clock	2.0 m	4.00 m ²
Multipath	1.0 m	1.00 m ²
Troposphere	0.5 m	0.25 m ²
UERE	~5.0 m	25.25 m ²

In our computations we assumed four parameters for the GPS-only and Galileo-only case: three coordinates and a receiver-clock bias; see *Section 23.3*. In the G2 constellation we assumed an additional GPS-Galileo time offset as parameter. With the choice of a unit covariance matrix of the observations, the DOP values are computed from the diagonal elements of the covariance matrix of the estimated parameters transformed to a local north-east-up frame:

$$\text{VDOP (1D)} = (\sigma_{up}^2)^{\frac{1}{2}};$$

$$\text{HDOP (2D)} = (\sigma_{north}^2 + \sigma_{east}^2)^{\frac{1}{2}};$$

$$\text{PDOP (3D)} = (\sigma_{north}^2 + \sigma_{east}^2 + \sigma_{up}^2)^{\frac{1}{2}}.$$

An indication of radial accuracy for 1D vertical, 2D horizontal, and 3D position is then given by:

$$\sigma_{up} = \text{UERE} \cdot \text{VDOP};$$

$$\sigma_{2D} = \frac{1}{\sqrt{2}} \text{UERE} \cdot \text{HDOP};$$

$$\sigma_{3D} = \frac{1}{\sqrt{3}} \text{UERE} \cdot \text{PDOP}.$$

Note that in the future GPS and Galileo measurements can be done on two civil frequencies. This means that the ionosphere will hardly contribute to the UERE any more, which will then reduce to about 2 m. However, strictly speaking, when we compute the DOP values in this case, we should include twice as many observations and introduce an ionospheric-delay parameter. This was not done in our computations. Also with EGNOS (European Geostationary Navigation Overlay Service) fully operational, the UERE should be reduced considerably as long as the signals of these satellites are not continuously blocked. *Figure 23.10* shows the distributions of PDOP, HDOP, and VDOP values under clear sky circumstances. Median values correspond to ratios of 0.5. The distribution of DOP values shows a long tail with a wider spread of DOP values higher than the median than DOP values smaller than the median. Especially for circumstances with high DOP values in the GPS-only and Galileo-only cases, the reduction of the DOPs in the G2 cases is large.

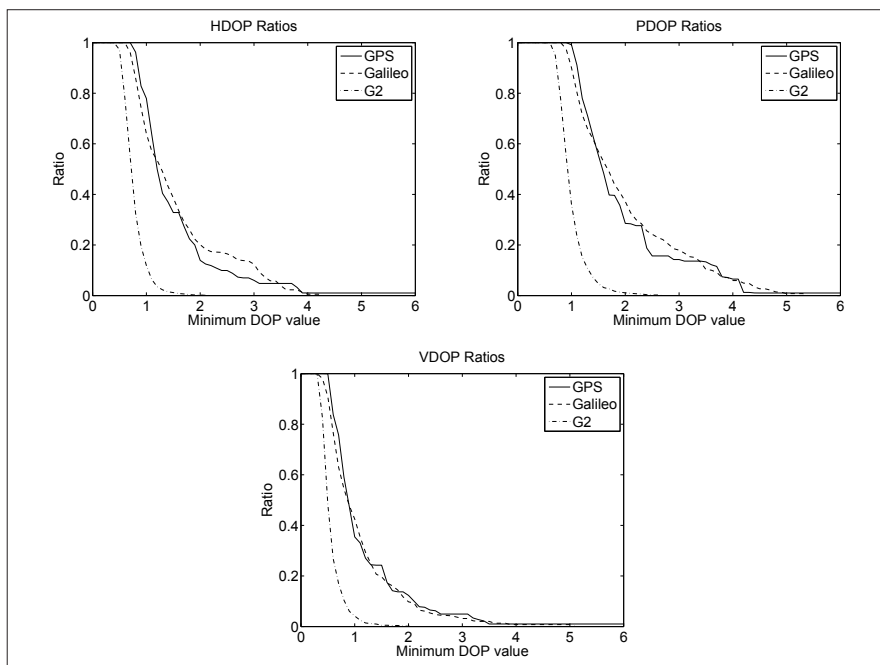


Fig. 23.10. DOP ratios for GPS, Galileo and G2 in case of a clear sky and an elevation cut-off angle of 10° for RD coordinates $x = 113400$, $y = 480250$. Based on 10 days of data, 1 epoch per minute.

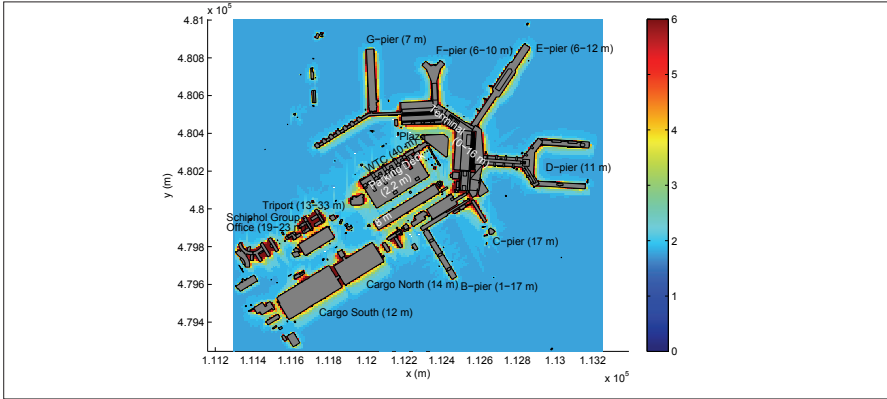


Fig. 23.11. Median GPS PDOPs at Schiphol Airport.

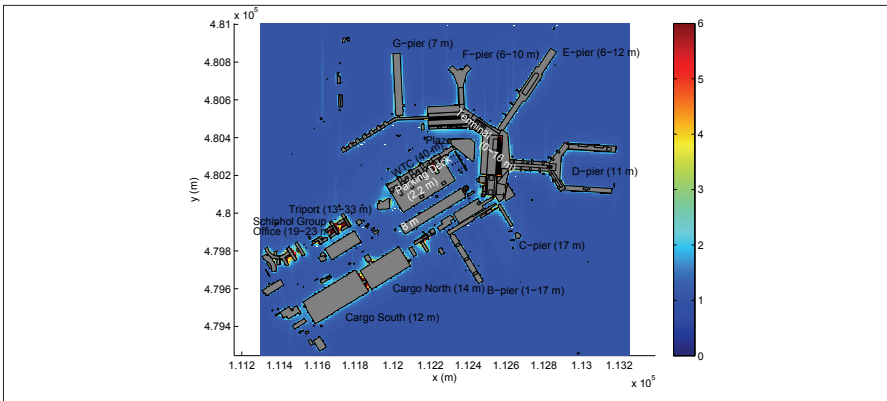


Fig. 23.12. Median G2 PDOPs at Schiphol Airport.

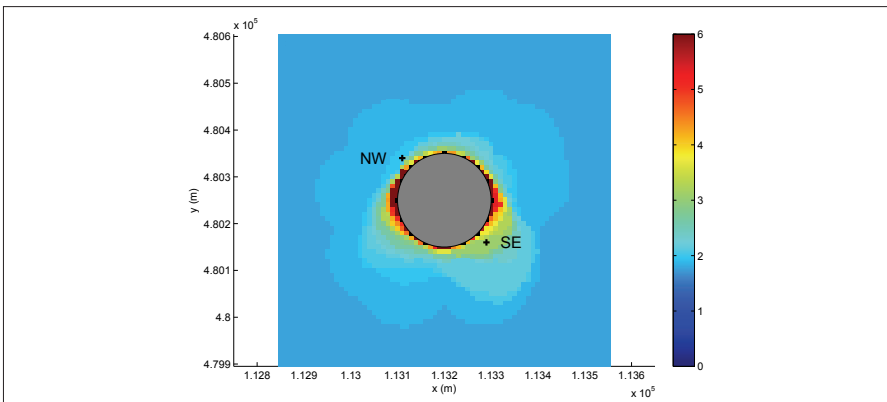


Fig. 23.13. Median GPS PDOPs around a (fictitious) 35-m high cylinder-shaped object of 200 m diameter at location Schiphol Airport. The north-west (NW) and south-east (SE) location are marked with +.

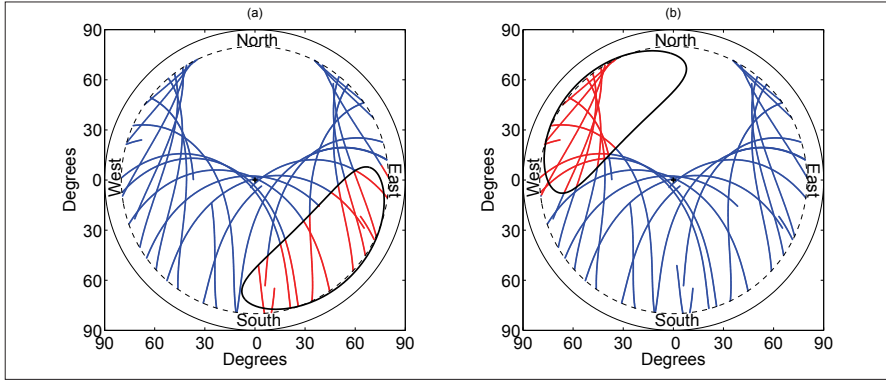


Fig. 23.14. GPS skyplots for the two locations indicated by + in *Figure 23.13*. Satellite positions are shown every minute for 12 hours. In blue are shown the satellites with unblocked LOS. In red the satellites blocked by the object. (a) the north-west (NW) location; (b) the south-east (SE) location.

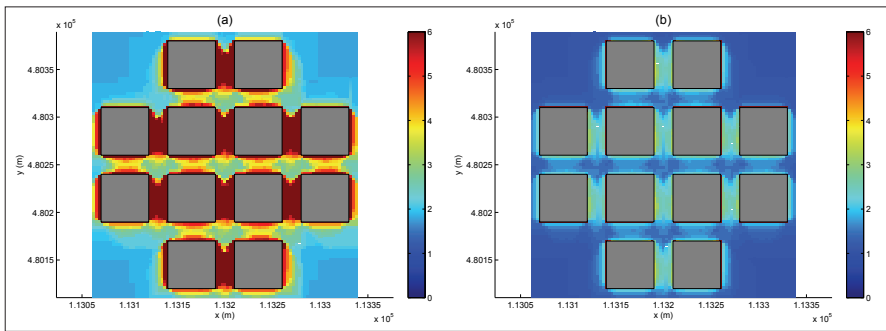


Fig. 23.15. Median PDOP values in the urban canyon model with parameters $l = 50$ m, $w = 20$ m, $H = 8$ m. (a) GPS only. (b) GPS and Galileo.

The median PDOPs over 96 epochs we computed at Schiphol Airport are given in *Figures 23.11* and *23.12*. Again the GPS and Galileo situation turned out to be very comparable (the latter is therefore not shown here), whereas the G2 situation gives a clear improvement. Also around the piers accuracy is clearly degraded in the GPS-only and Galileo-only situation.

Especially notable are the southern ‘cast shadows’ of the cargo buildings. Because of the hole in the satellite coverage in the north one would expect this shadow to be more clearly present in the north than in the south. Larger shadows on the south side than on the north side can also be seen for some of the piers, e.g. the E-pier. Because this is unexpected, we constructed a simple model of a 35 m high cylinder-shaped object and 200 m diameter in a further empty area at the Schiphol location. If there would be a symmetrical satellite coverage, the cast shadows should be equal in all

directions. *Figure 23.13* shows the median GPS PDOPs for the same 96 epochs as used for the Schiphol computations. This figure tells that the shadow is not so much in the south direction but in the south-east and south-west direction. To rule out the possible effect of a heterogenous satellite distribution caused by a limited amount of epochs, we repeated the computation for two locations shown in *Figure 23.13* indicated by a + sign for every minute during 12 hours. *Figure 23.14* shows the skyplots for these locations. For the latter computation we found median GPS PDOPs of 1.90 and 2.95 instead of previously found values of 1.89 and 2.97 of the north-west and south-east locations respectively, thus ruling out that the limited amount of 96 epochs was an issue. The amount of LOSs blocked by the cylinder turned out to be 4724 and 5009 respectively. So we saw more satellites in the north-west than in the south-east causing the lower median PDOP values in the north-west, although that is also where more outliers of high PDOP values were actually found. Although there is a clear hole in the satellite coverage in the exact north the density of satellites in the north-west (and north-east) is higher than in the southern directions, thus causing lower median PDOPs in the north.

The median PDOPs computed for the urban canyon model are shown in *Figure 23.15*. We restricted ourselves to one set of relatively mild conditions. Notable are the high median PDOP values in north-south direction for the GPS-only case. Since availability under these circumstances is low (an insufficient amount of satellites results in a PDOP of infinity) the median values are often larger than 6. For presentation purposes the locations with insufficient availability are indicated with the same colour as a median PDOP of 6. In the G2 case in north-south streets the median PDOPs are at a much more acceptable level.

23.5 Conclusions

GNSS availability in urban areas is seriously degraded by buildings blocking LOSs from more than one side. Only under mild conditions 95% availability can be reached. For our mid-latitude computations this was the case for, e.g., 20 m wide streets surrounded by 8 m-high buildings, but only in east-west streets or on squares, but not close to buildings. In the G2 situation substantial improvements in availability (30%–50%) can be made for those situations where availability is above ~10% for GPS only. This means that for mild conditions, like 20 m wide streets surrounded by 8 m high buildings, 95% availability can be reached anywhere. But still, under more difficult conditions 95% cannot be reached everywhere and anytime in urban canyons. In a constellation with three GNSSs, including the Russian GLONASS, the availability improvement should be even higher. But it is unexpected that this will lead to 95% availability everywhere and anytime. In areas with buildings on one side, like the piers of Schiphol Airport,

95% availability can be reached with GPS (and Galileo) only. The (time) median accuracy of the determined coordinates obtained from GNSS single-epoch observations in those situations can however degrade by up to a factor three. In the G2 situation the DOPs will be about a factor two better, and, with two civil frequencies for both GPS and Galileo, the accuracy will improve even further. This means that even close to buildings an accuracy under the 10 m (a mismatch of 10 m or lower, 95% of the time), as is often required for LBS, can be achieved in the future, although one should realize that there can be other blocking objects with a deteriorating effect that we have not considered. Under more difficult conditions in urban canyons, GNSS positioning should at least involve using a history of measurements, e.g. by applying Kalman filtering techniques, or additional information from, e.g., inertial navigation or other observations.

Acknowledgements

This research was part of the Bsik project RGI-150 (Ruimte voor Geo-Informatie) *3D positioning infrastructure in the built-up environment*. We thank Dick Viveen of the Schiphol Group for his cooperation and for providing the Schiphol data set.

References

- Bowring BR (1976) Transformation from spatial to geographical coordinates, *Survey Review*, 23, pp. 323–327.
- Bradbury J (2007) Prediction of urban availability and signal degradation using virtual reality city models, ION GNSS 2007, Fort Worth, Texas.
- Bradbury J, Ziebart M, Cross PA, Boulton P, Read A (2007) Code multipath modelling in the urban environment using large virtual reality city models: Determining the local environment, *Journal of Navigation*, 60, pp. 95–105.
- Hofmann-Wellenhof B, Lichtenegger H, Collins J (1992) *GPS: Theory and practice*, Springer-Verlag, Wien, 3rd edn.
- Liu G, Zhang K, Densley L, Wu F, Retscher G (2006) High fidelity 3D urban model-based signal performance simulation of the current and future GNSS in Australia, IGNSS Symposium, Holiday Inn Surfers Paradise, Queensland, Australia.
- Min EJ de (1996) *De geoïde van Nederland*, PhD thesis, Delft University of Technology, the Netherlands.
- Odijk D, Kleijer F (2007) Performance of high-sensitivity GPS for personal navigation at Schiphol Airport, the Netherlands, IGNSS Symposium, Sydney, Australia.
- Odijk D, Kleijer F (2008) Can GPS be used for location-based services at Schiphol Airport, the Netherlands?, *Proceedings of the 5th Workshop on Positioning, Navigation and Communication 2008*, Hannover Germany, pp. 143–148.

- Schreutelkamp FH, Strang van Hees GL (2001) Benaderingsformules voor de transformatie tussen RD- en WGS84-coördinaten, *Geodesia*, pp. 64–69.
- Sleewaegen JM, Boon F (2001) Mitigating short-delay multipath: A promising new technique, *ION GPS 2001*, Salt lake City, Utah.
- Swann J, Chatre E, Ludwig D (2003) Galileo: Benefits for Location Based Services, *Journal of Global Positioning Systems*, 1, pp. 58–66.
- Taylor G, Li J, Kidner D, Brunson C, Ware M (2007) Modelling and prediction of GPS availability with digital photogrammetry and LiDAR, *International Journal of Geographical Information Science*, 21, pp. 1–20. DOI: 10.1080/13658810600816540.
- Tiberius C, Verbree E (2004) GNSS positioning accuracy and availability within Location Based Services: The advantages of combined GPS-Galileo positioning. In: 2nd ESA/Estec workshop on Satellite Navigation User Equipment Technologies, G.S. Granados (Ed), ESA publications division, Noordwijk, pp. 1–12.
- Verbree E, Tiberius C, Vosselman G (2004) Combined GPS-Galileo positioning for location based services in urban environment, In: *Proceedings of the Location Based Services & Telegraphy Symposium 2004*, Austria, Vienna University of Technology, pp. 99–107.
- Verhagen S (2002) Innovation Studying the performance of Global Navigation Satellite Systems: A new software tool, *GPS World*, 13, pp. 60–65.
- Walker JG (1984) Satellite constellations, *Journal of the British Interplanetary Society*, 37, pp. 559–571.